Journal of Mathematical Chemistry 9(1992)161–180

THE MATHEMATICAL MODELLING OF CLUSTER GEOMETRY

Ian BYTHEWAY and David L. KEPERT
Department of Chemistry, University of Western Australia, Nedlands, 6009, W.A., Australia

Received 30 July 1991

Abstract

Calculations of minimum energy configurations for aggregates of up to forty atoms, commonly referred to as clusters, are presented. In contrast to previous studies, random initial configurations have been optimised to find the lowest energy structure for a given number of atoms. Three different two-body, bireciprocal potential functions were used in these calculations and in the case of the Lennard–Jones potential, previously calculated results have been confirmed. New structures obtained using softer potentials are also presented. Minimum energy structures of small clusters containing two different types of atoms have also been calculated, and the relationship between the geometry of a cluster and the relative sizes of its constituent atoms examined.

1. Introduction

This paper is concerned with the description of the geometries of chemical species often referred to as clusters. A cluster may be defined as an aggregate of atoms, ions or molecules intermediate between the single, isolated species and the bulk material. The study of cluster geometry can be simplified by considering it in terms of the more general problem of the most efficient packing of spheres.

Studies of sphere packing have yielded several results of importance to cluster geometry. Limits for the maximum density of a closest packed volume of space have been calculated [1] and it has been shown [2] that the local density of close packed regions may exceed that for an infinite close packed array, although such regions cannot be extended *ad infinitum*. Also of relevance to the study of cluster geometry was the discovery [3] that spheres packed in an icosahedral manner have a packing density close to that for the close packed cuboctahedron.

Calculations of cluster geometry were pursued after experimental results showed that small aggregates of atoms did not have close packed structures [4–6]. These were performed using a two-body potential [6] in which the geometry of an aggregate of atoms is described in terms of the individual atom–atom interactions, viz.:

$$E = \sum_{i>j}^{i=N} V(r_{ij}), \tag{1}$$

where N is the total number of atoms in the cluster and $V(r_{ij})$ is a function relating the distance between two atoms to the energy of their interaction. Further calculations of this type showed that the 13 and 55 atom icosahedron is energetically more favourable than the corresponding cuboctahedron [7]. This result is similar to those obtained from the study of random packing [8–12] and demonstrated that geometries with fivefold symmetry may be preferred over the more conventional close packed arrangements.

The first systematic calculations of minimum energy cluster conformations were performed by Hoare and coworkers [13–16]. They showed that the minimum energy configurations of small assemblies of atoms are not based on cubic close packing and often contain icosahedra or pentagonal symmetry. Minimum energy cluster geometries were calculated using a growth sequence, in order to avoid the computational demands of searching for global minima. In such calculations a minimum energy, N-atom cluster can be used as a "seed" from which the $N+1$ atom cluster can be constructed, minimized (or "relaxed") and then used as a seed for the next cluster, and so on. This method of calculation does not guarantee that global minimum energy structures will be found. However, the clusters generated using these algorithms were calculated to be of lower energy than the corresponding close packed structure, and pentagonal symmetry and icosahedra were found to be important motifs in these minimum energy configurations, despite the fact that neither can be used to fill large volumes of space efficiently.

Other calculations of cluster geometry which do not use a growth algorithm have been carried out. Minimum energy clusters containing up to 25 atoms, using an optimisation algorithm based upon simulated annealing, have been used [17]. A larger study, using a lattice-based search and optimisation procedure, was performed and minimum energy clusters containing up to 147 atoms were calculated. In both of these studies, many of the structures obtained are of lower energy than those proposed previously [16]. Recently, rearrangement mechanisms and transition state geometries have been proposed for small clusters ($N \leq 150$) [18] and possible cluster-growth schemes investigated.

The calculations presented in this paper are concerned with minimum energy configurations of atomic clusters. In the light of previous results [13–19], it was decided that the dependence of the starting configuration on the final cluster geometry should be considered. Consequently, a systematic search for global minima, resulting from the optimisation of random starting geometries, has been performed in order to find the lowest energy configurations of small clusters.

2. Method of calculation

Minimum energy configurations of atomic clusters have been calculated using three pair potentials of the general form:

$$V(r_{ij}) = \frac{1}{r_{ij}^{2n}} - \frac{2}{r_{ij}^{n}}, \tag{2}$$

where the values 6, 4 and 1 have been used for n. These will be referred to as the 12–6, 8–4 and 2–1 potential functions, respectively. This form of the potential function was chosen so that the minimum value of the function occurs when the separation between atoms is unity (see fig. 1). Summation of the pair-interaction energies, as described in (1), gives the total energy of any arrangement of atoms.

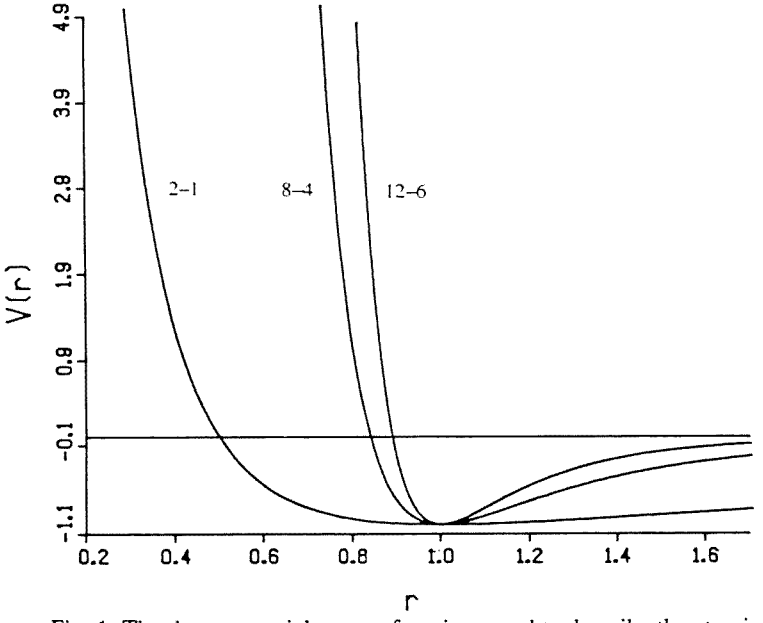

Fig. 1. The three potential energy functions used to describe the atomic interactions in the calculation of minimum energy cluster configurations.

Random starting configurations were optimised using a "steepest descent" optimisation algorithm developed by Davidson [20] and modified for use by this research group [21–23]. Derivatives were calculated analytically for each of the $3N - 6$ variables while six of the atomic coordinates were set to zero to avoid the calculation of rotational and translational isomers. No symmetry was imposed on the structure during these calculations.

This method of calculation was computationally demanding, and a large number of random initial configurations were used in order to find the lowest energy cluster geometry (as many as 2500 for the 12–6 potential and approximately 100 to 500 for the 8–4 and 2–1 potentials). This methodology does not assure that a global minimum energy structure will be obtained, but previous work done by this research group [23,24] has proved successful and it was thought that useful results would be obtained by proceeding in this manner.

3. Results of calculations performed using the 12–6 potential

Minimum energy cluster geometries were calculated using the Lennard–Jones, 12–6 potential by minimising random starting configurations. The energies of the lowest energy structures are in agreement with those of Northby [19], although as the cluster size was increased, the frequency with which this geometry was obtained decreased (see table 1). For even larger clusters, the lowest energy structures described by Northby [19] were not found, due to the increase in the number of deep local minima.

The geometries obtained from these calculations show that minimum energy geometries can be constructed by the packing of centred-icosahedral subunits, the stability of which is well established [16]. Representative examples of this are shown in fig. 2, for clusters consisting of 19, 23, 26 and 29 atoms. Each of these clusters can be constructed by the fusing of centred-icosahedra so that the shape has a conventional overall symmetry while still retaining some of the features unique to icosahedral packing.

4. Results of calculations performed using the 8–4 potential

A slightly softer potential, when $n = 4$ in eq. (2), was also used to see how changing the interatomic potential function would change the minimum energy cluster geometry. For clusters containing up to 27 atoms, there was no difference between structures obtained using either of the 12–6 or 8–4 potentials. However, for clusters containing more than 27 atoms, different geometries were calculated, lower in energy than if the previously obtained solutions from the 12–6 potential calculations were used as starting approximations.

The difference in geometries between the two sets of calculations is due to the manner in which the sites about a central double icosahedron were filled. Examples of minimum energy geometries, showing this systematic filling of sites about a central double-icosahedron culminating in the D_{5d}, $N = 34$ cluster, are shown in fig. 3. It is interesting to note that the $N = 29$ geometry was the same for both sets of calculations and that the $N = 34$ structure was previously suggested as a minimum energy structure for the 12–6 potential [13].

Clusters containing up to 40 atoms, calculated using this potential function as minima, were obtained with greater confidence than in the previous case, as can be seen in table 1. These minima were obtained slightly more frequently and took less time to calculate, although it is still possible that the calculated geometries do not represent global minima.

The minimum energy geometries of some larger clusters are shown in fig. 4. An increase in the number of atoms fully encapsulated within the cluster boundary can be seen for these larger clusters. The largest cluster calculated, consisting of 40 atoms, can be described as an uncentred icosahedron surrounded by an incomplete dodecahedral framework. This is an important structure since it can be related to

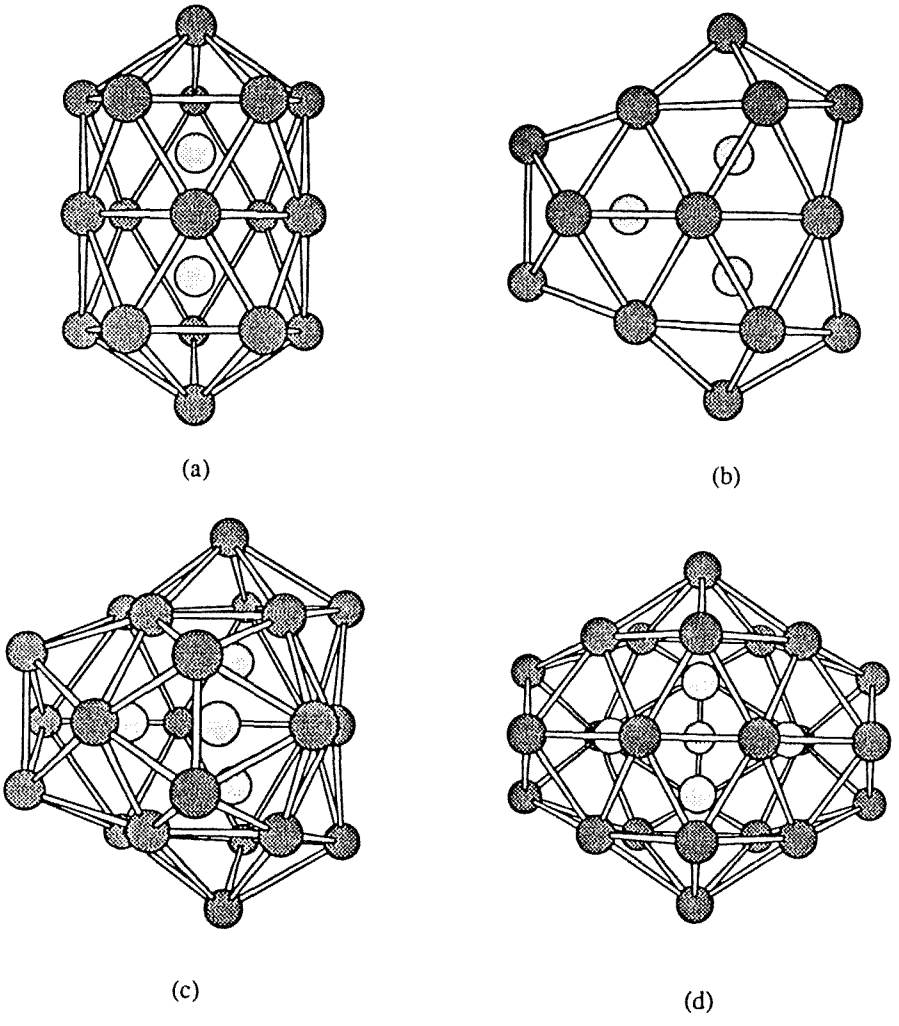

Fig. 2. Minimum energy cluster geometries calculated using the 12–6 interatomic potential function. In this and subsequent figures, atoms fully enclosed within the cluster are shown with a different shading pattern and non-bonded for the sake of clarity. (a) The $N = 19$, D_{5d} double-icosahedron. (b) The $N = 23$, D_{3d} tri-icosahedron. (c) The $N = 26$, T_d tetra-icosahedron. (d) The $N = 29$, D_{3d} penta-icosahedron.

the $N = 55$ Mackay icosahedron [3], expected to be the minimum energy geometry for a cluster of 55 atoms [19]. Calculations were not performed for clusters containing greater than 40 atoms due to the increased computational requirements for the location of global minima.

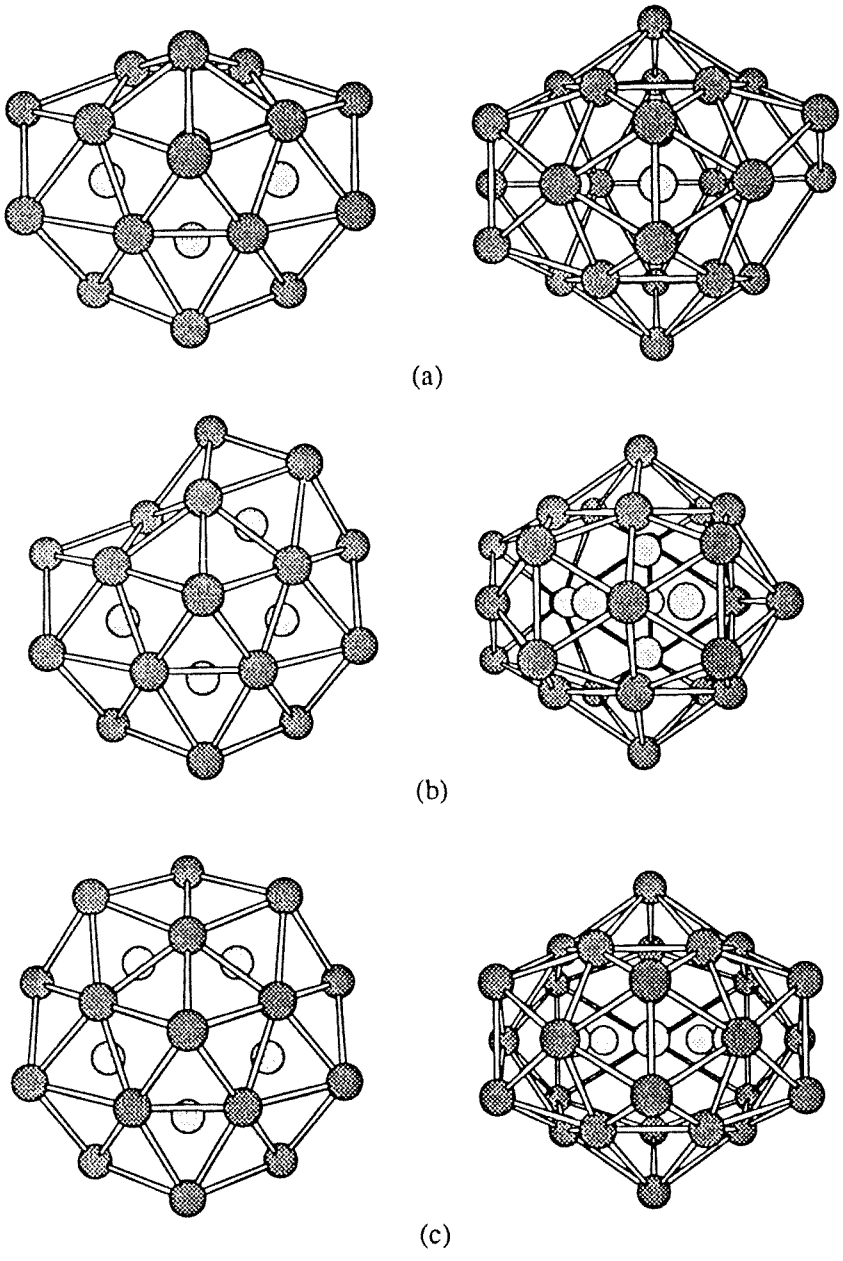

Fig. 3. Some minimum energy cluster geometries calculated using the 8–4 interatomic potential function. (a) Two views of the $N = 28$ cluster, different to that obtained using the 12–6 interatomic potential function. (b) Two views of the $N = 32$ cluster. Note the systematic filling of sites about the central double-icosahedron. (c) Two views of the D_{5d} 34-atom cluster; the sites about the central double-icosahedron are now fully occupied.

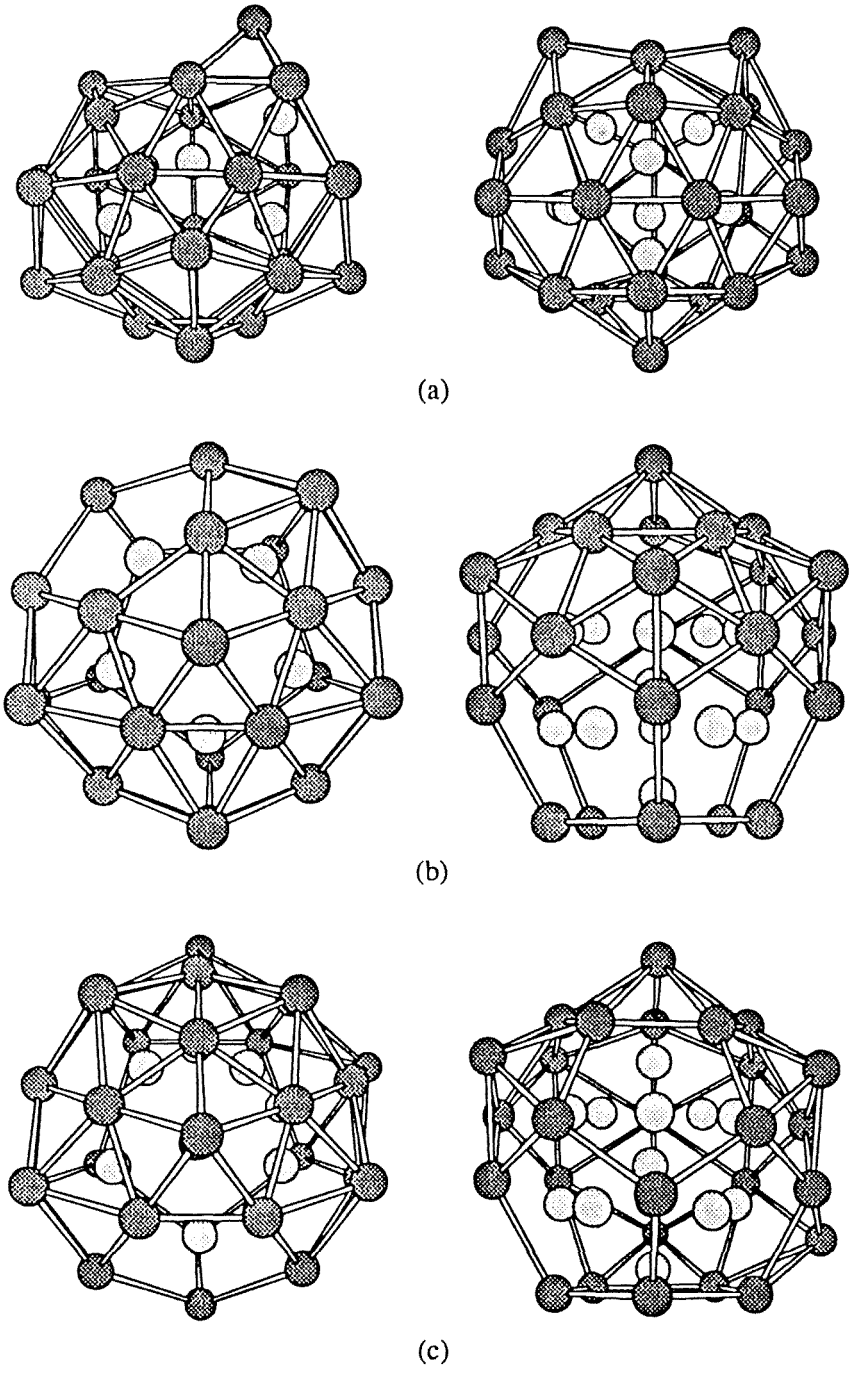

Fig. 4. Some minimum energy cluster geometries calculated using the 8–4 interatomic potential function. (a) Two views of the $N = 36$ geometry, shown looking down the pseudo-C_5 axis of the double icosahedral framework and viewed perpendicular to this axis, showing extra capping atoms. (b) Two views of the $N = 38$ geometry, shown looking down the C_5 axis of the icosahedral core of enclosed atoms and shown perpendicular to this. (c) Two views of the $N = 40$ geometry, the minimum energy structure shown looking down the approximate C_5 axis of the enclosed icosahedron and shown perpendicular to this.

5. Results of calculations performed using the 2–1 potential

The softest interatomic potential function used to calculate cluster geometry was the 2–1 potential, that is, when $n = 1$ in eq. (2). This potential function has been used previously to calculate the structures of boron hydride molecules [25–27] and it was decided that its use would further test the effect of the interatomic potential used upon the minimum energy geometry.

Global minima were obtained more frequently than in the two preceding sets of calculations and in most cases calculated geometries are quite different to those obtained previously. In general, the tendency for geometries to be based upon the icosahedron were not calculated, for example the $N = 9$ cluster was calculated to be a bicapped pentagonal bipyramid using the harder potentials, but was calculated to be a tricapped trigonal prism using this potential function. Exceptions to this are the geometries obtained for the $N = 3$–7, 13, 23, 26 and 29 clusters, which are the same as those calculated using the 12–6 and 8–4 potentials.

The geometries calculated for $N = 14$–19 clusters are not based upon the capping of the faces of the centred-icosahedron, as found in the previous calculations. Instead, additional atoms add to the cluster and are in contact with the central atom, which results in different structures. A good example of this is the $N = 15$ cluster (fig. 5(a)) which is a bicapped, centred hexagonal antiprism and not a bicapped centred icosahedron as was previously calculated. Similarly, the $N = 17$ cluster is a {1, 6, 1, 6′, 3} polyhedron (fig. 5(b)), and the $N = 18$ cluster (fig. 5(c)) contains two enclosed atoms, at a cluster size one less than calculated using the harder potentials. In general, clusters calculated using the 2–1 potential contain more encapsulated atoms than those calculated using the harder 12–6 and 8–4 potentials.

A tetrahedron of atoms is encapsulated within the $N = 24$ structure (fig. 6(a)), although the structure does not have overall tetrahedral symmetry as does the $N = 26$ structure calculated using the 12–6 potential, which also contains a tetrahedral core of atoms. This lack of relationship between the symmetry of the core and the outer shell of atoms can also be seen in the $N = 28$ cluster (fig. 6(b)) which contains an enclosed octahedral core, a core polyhedron not previously calculated to be an energy minimum. The $N = 30$ structure (fig. 6(c)) is perhaps the best example of the difference in orientation between the core and outer shell of the cluster. This cluster consists of an octahedron surrounded by atoms which form a snub cube [28], although the symmetry axes of both structures are not coincident.

This somewhat unexpected feature is observed in the clusters with $N = 30$–34 atoms; again the orientation of the inner core is unusual with respect to the arrangement of the atoms on the outer surface of the cluster (fig. 7(a)). Although the symmetry of the enclosed octahedron is obvious, it is not reflected in the arrangement of the outer shell of atoms. In each of these structures, regions of five- and six-coordination exist and the structures are of a similar nature to those obtained for soft packing [8,29].

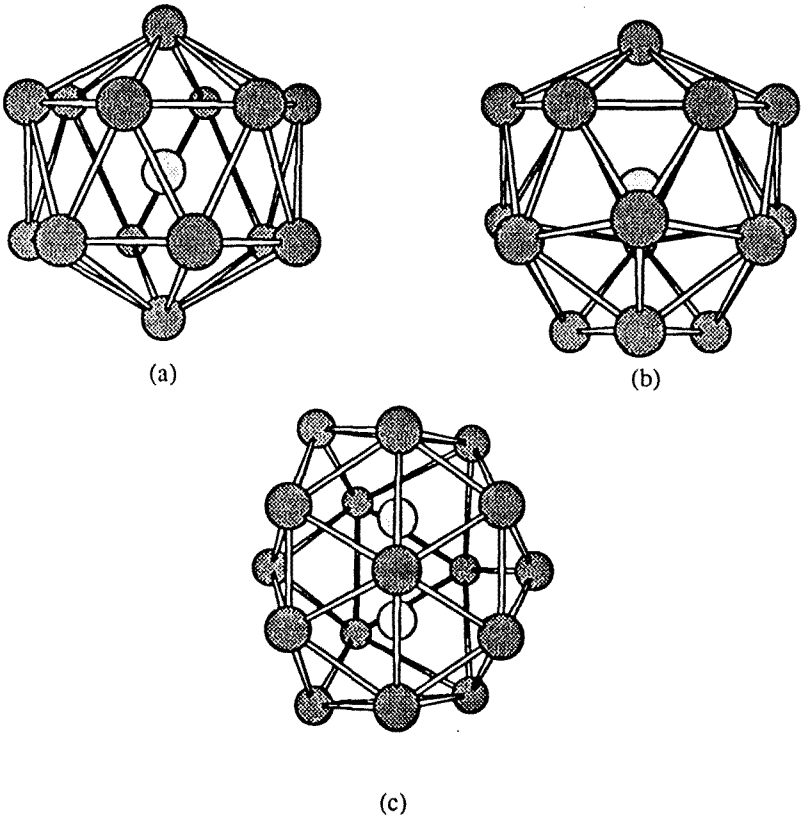

Fig. 5. Cluster geometries calculated using the 2–1 interatomic potential function. (a) The $N = 15$ structure. A bicapped, centred hexagonal antiprism. (b) The {1, 6, 1, 6′, 3} polyhedron calculated for the $N = 17$ cluster. (c) The $N = 18$ cluster showing two encapsulated atoms.

As cluster size is increased, so too is the number of six-coordinate atoms on the cluster surface, evident in the $N = 39$ structure (fig. 7(b)) and the formation of an almost-square face, instead of adjacent pentagonal faces, has occurred. The structure calculated for $N = 40$ (fig. 7(c)) is quite unusual since there is an uncapped pentagonal face in this structure. Its core polyhedron is distorted from the ideal tricapped trigonal prism and does not possess a C_3 axis. In the $N = 40$ cluster, a core atom is close to the uncapped pentagonal face, forming an inverted cap and maximum connectivity is preserved. Calculations beyond $N = 40$ were not performed, although it is likely that global minima could still be found with confidence; however, as was the case for the previous calculations, there is an increase in the number of local minima found with the increase in cluster size.

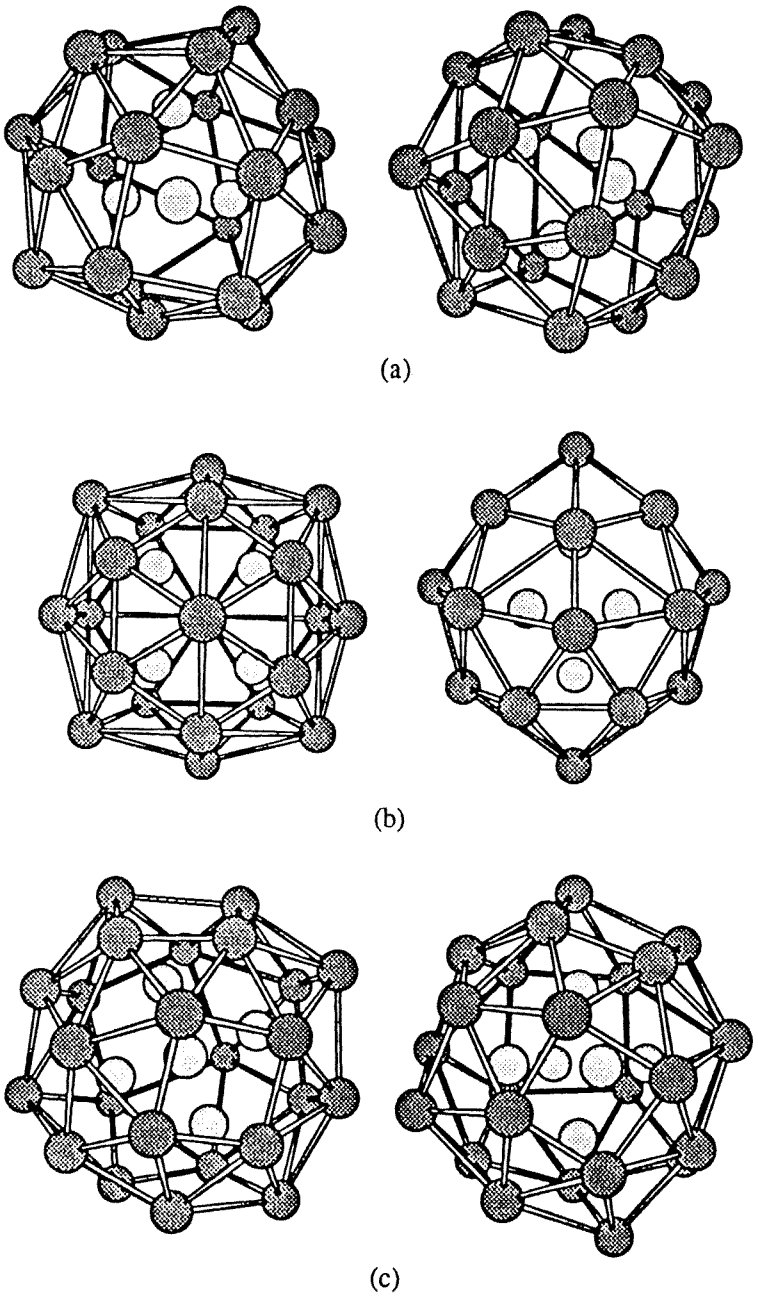

Fig. 6. Minimum energy structures calculated using the 2–1 potential. (a) Two views of the $N = 24$ structure showing the enclosed tetrahedron of atoms. (b) Two views of the $N = 28$ cluster which contains an encapsulated octahedron. Note the orientation of the core to the outer shell of atoms. (c) Two views of the $N = 30$ structure, an octahedral core surrounded by a shell of atoms arranged in the shape of a snub cube.

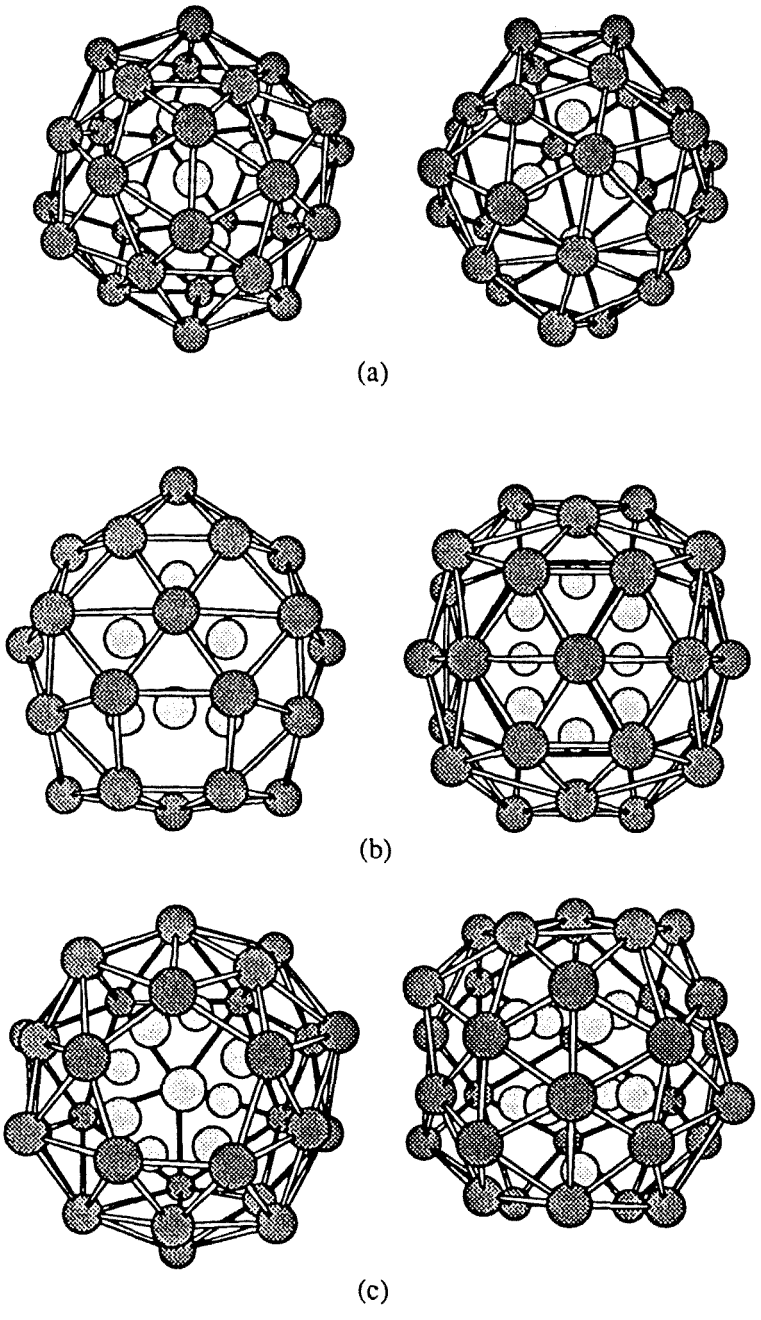

Fig. 7. Larger cluster geometries calculated using the 2–1 potential. (a) Two views of the $N = 34$ cluster. Note the arrangement of the outer shell with respect to the encapsulated octahedron. (b) Two views of the $N = 39$ cluster showing the tricapped trigonal prism of core atoms. (c) Two views of the $N = 40$ structure showing the uncapped pentagonal face and distorted tricapped trigonal prism of core atoms.

6. Geometries of clusters containing two different types of atom

A logical continuation of the work described in the previous section is to consider the minimum energy configurations of clusters composed of more than one type of atom. This is chemically sensible and clusters of this type are known [30–33]. The method of calculation used was essentially the same as that described above, except that three potentials governing the atom–atom interactions within the cluster were required. These functions were used to account for the X–X, Y–Y and X–Y interactions within a cluster consisting of X and Y type atoms, that is, the cluster is of the general type X_xY_y. Cluster sizes from $N = 13$ to 19 for various combinations of X and Y atoms have been studied (where $N = x + y$). The structures obtained from the previous calculations, suitably substituted, were used as starting approximations for the calculations. In addition, calculations using random starting approximations were done to establish that the lowest energy structures were found. The potential functions used to describe the interactions between the two different types of atom were of the general Lennard–Jones type. This avoids the complication of deciding upon new types of potential functions to model the atomic interactions and allows for comparison with the calculations already presented.

The first of the calculations were performed using potential functions in which the minimum energy occurred at r values of 0.8, 0.9 and 1.0 for Y–Y, X–Y and X–X interactions, respectively. The potential functions which give these minima are:

$$V(r_{ij}) = \frac{0.06872}{r_{ij}^{12}} - \frac{0.52429}{r_{ij}^{6}} \qquad Y-Y \text{ interactions,} \tag{3}$$

$$V(r_{ij}) = \frac{0.28243}{r_{ij}^{12}} - \frac{1.06288}{r_{ij}^{6}} \qquad X-Y \text{ interactions,} \tag{4}$$

and the 12–6 potential described in section 3 was used to model X–X interactions.

Substituted 13-atom clusters were first studied using this set of interatomic potentials and, not surprisingly, it was found that the smaller Y atom preferentially occupies the central position of the icosahedron. This is expected since the centre-vertex distance is about 0.95 of the vertex–vertex length. It was also found that as the degree of substitution in the cluster increased, the minimum energy structures were those in which the Y atoms occupied sites close together, that is, Y atoms tended to congregate and form a subcluster within the framework of the larger cluster.

The calculated minimum energy geometries of the majority of clusters studied were not significantly different to the parent, unsubstituted cluster. However, the substituted $N = 16$ atom cluster shows some eclipsing of the plane of atoms capping the icosahedron (fig. 8(a)) and the structure of the substituted 17-atom cluster was different to the parent cluster. The minimum energy $N = 17$ cluster is unusual since

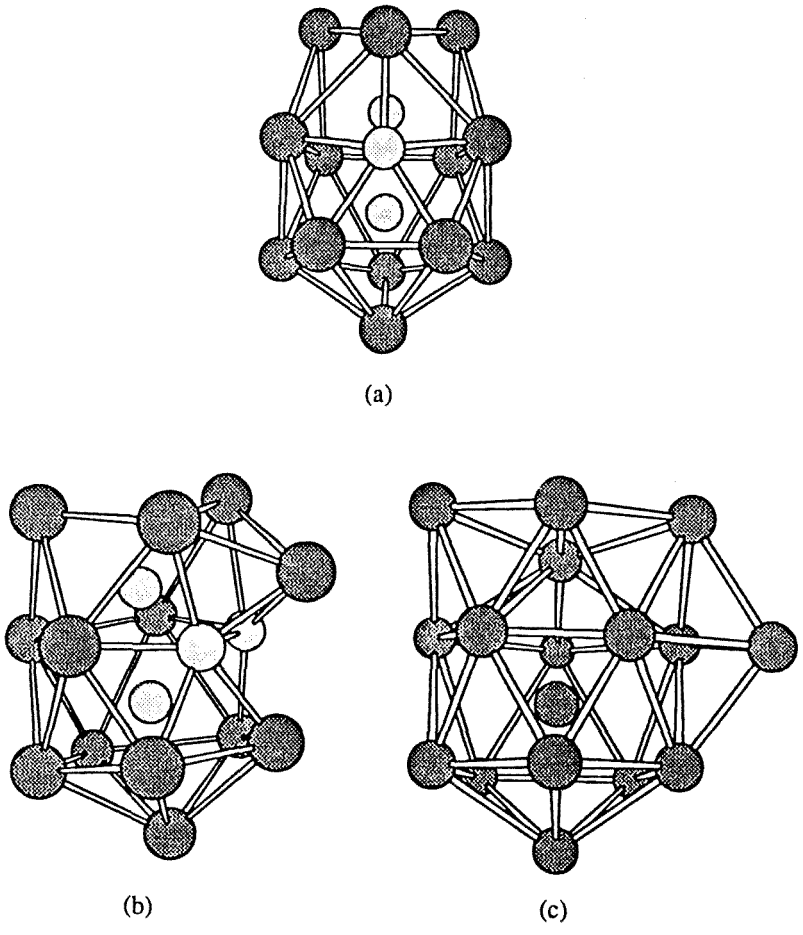

Fig. 8. The minimum energy geometries of some substituted clusters calculated when the size of the Y atom is 0.8 of the size of the X atom. In this and subsequent pictures of substituted clusters, the Y atoms are shaded differently, and for the sake of simplicity are drawn without nearest-neighbour contacts. (a) The minimum energy geometry of the $X_{13}Y_3$ cluster showing the eclipsed plane of capping atoms. (b) The $X_{13}Y_4$ cluster showing the Y atoms in the plane above the icosahedron; the analogous unsubstituted cluster is also shown for comparison.

it does not follow the growth scheme expected from the addition of atoms to the icosahedron culminating in the double-icosahedron [14,17,19,34]. In contrast, and as a consequence of the shorter $X-Y$ and $Y-Y$ equilibrium distances in the substituted cluster, the 17-atom minimum energy $X_{13}Y_4$ cluster has a geometry closer to that expected if the previously suggested [13] growth scheme was followed (fig. 8(b)). These represent the only anomalies for this set of calculations, and so clusters

containing more than 19 atoms were not studied; instead, the ratio of the size of X with respect to Y was increased to see if this had any effect on cluster geometry.

A rather more extreme difference in X and Y atom sizes was used in these calculations; the radii of Y atoms were treated as being half that of the X atoms. Such a large difference in atom sizes is perhaps unrealistic, the only cases for which they may be valid would probably involve ionic species and it is doubtful that a Lennard–Jones potential would describe the interactions between such species. However, the preference for the formation of Y atom subclusters calculated above can be tested and new minimum energy structures may be calculated. In particular, the relationship between atom size and the formation of structures with pentagonal symmetry can be further examined.

The $X-Y$ and $Y-Y$ interatomic potentials used were:

$$V(r_{ij}) = \frac{1}{(2r_{ij})^{12}} - \frac{2}{(2r_{ij})^{6}} \qquad Y-Y \text{ interactions,} \tag{5}$$

$$V(r_{ij}) = \frac{0.031673}{r_{ij}^{12}} - \frac{0.3559571}{r_{ij}^{6}} \qquad X-Y \text{ interactions,} \tag{6}$$

and the same potential as described above was used for the $X-X$ interactions. Because of the large number of possible calculations, only those for the substitute 19-atom cluster were performed.

The calculations were performed in the same manner as described above. A substituted double-icosahedron was used as the starting approximation; however, the presence of much smaller Y atoms resulted in very different minimum energy structures and random starting approximations were also used to check whether or not the minima found indeed had the lowest energies. In most cases, the double-icosahedral starting approximation yielded only local minima.

Those minimum energy clusters which have interesting structures will be considered, the first of which is $X_{16}Y_3$ (fig. 9(a)) which has a mirror plane but is very different to the double-icosahedron. The smaller Y atoms in this cluster are encapsulated within an outer shell of X atoms, as is the case for the structure of the $X_{15}Y_4$ cluster (fig. 9(b)). The tendency of the Y atoms to form subclusters, as found in the other calculations of X_xY_y clusters above, is seen in all of the clusters calculated when the Y atom is half the size of the X atom. This is no more evident than in the $X_{13}Y_6$ cluster (fig. 9(c)), in which the Y atoms form an octahedron about which the X atoms are distributed, in a manner analogous to that calculated by this group [24] for a minimum energy stereochemistry of $M_6(CO)_{13}$ (fig. 9(d)).

The structure of the $X_{12}Y_7$ cluster (fig. 10(a)) is interesting since the Y atoms do not form a pentagonal bipyramid as might have been expected; rather they form a capped octahedron. This tendency to form structures in which the Y atoms have a geometry based on the octahedron, and not the pentagonal bipyramid, is also seen

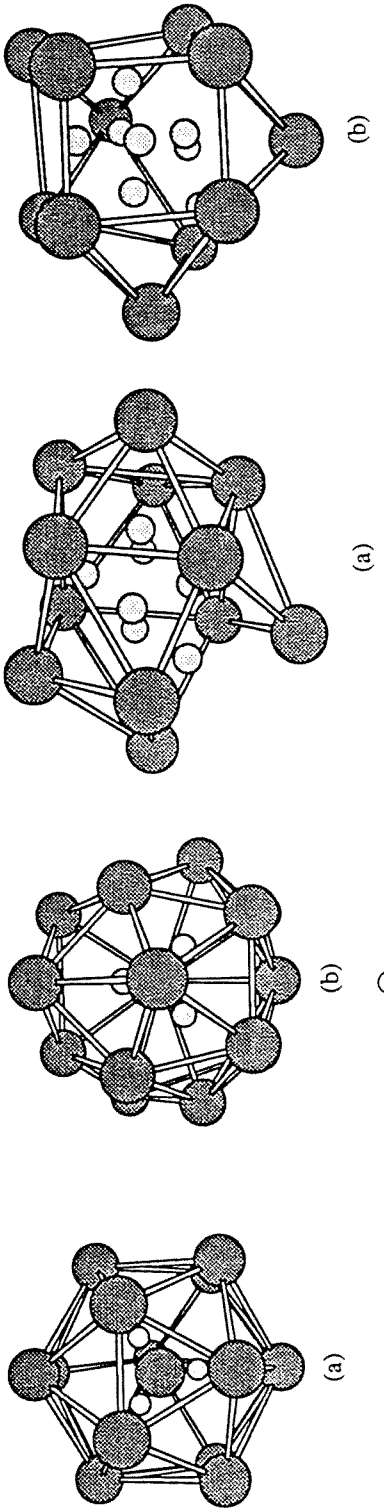

Fig. 9. The minimum energy geometries of some substituted clusters calculated when the size of the Y atom is half the size of the X atom. (a) The $X_{16}Y_3$ cluster showing a mirror plane and the encapsulated triangle of Y atoms. (b) The bicapped icosahedron of X atoms surrounding an enclosed tetrahedron of Y atoms, the geometry for the $X_{15}Y_4$ cluster. (c) The $X_{13}Y_6$ cluster, which consists of an octahedron of Y atoms surrounded by X atoms. (d) The minimum energy stereochemistry calculated for $M_6(CO)_{13}$ [24].

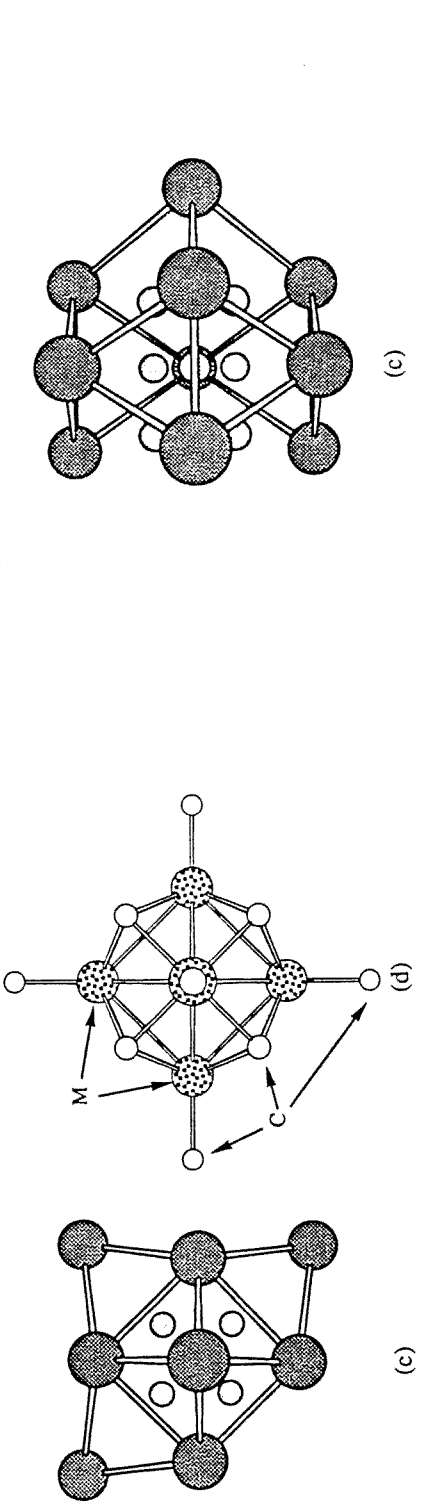

Fig. 10. The minimum energy geometries of some substituted clusters calculated when the size of the Y atom is half the size of the X atom. (a) The $X_{12}Y_7$ cluster which contains a capped octahedron of Y atoms and not the pentagonal bipyramid as might have been expected. (b) The $X_{11}Y_8$ cluster showing the bicapped octahedron of Y atoms. (c) The $X_{10}Y_9$ cluster which has the Y atoms arranged in the shape of two face-sharing octahedra and an outer polyhedron of X atoms which is almost an anticuboctahedron.

in the structure of the $X_{11}Y_8$ cluster (fig. 10(b)) in which the Y atoms are arranged in a bicapped octahedron. Following this trend, the $X_{10}Y_9$ cluster (fig. 10(c)) contains two face-sharing octahedra of Y atoms, surrounded by an almost anticuboctahedral arrangement of X atoms.

7. Conclusion

Minimum energy geometries for several types of clusters have been studied. The shape of clusters containing N similar atoms ($3 \leq N \geq 40$) have been calculated using three different bireciprocal potential functions. Configurations of clusters which contain two different types of atom have also been calculated (for $N \leq 19$ atoms) using modified 12–6 potentials to model the different types of atom–atom interactions. In each calculation, all $3N-6$ positional variables were treated independently without the imposition of any symmetry. For each cluster, many random starting approximations were minimised in order to find the lowest (and hopefully global) energy structure. For the 2–1 and 8–4 potential functions, this proved successful, with the lowest energy structure occurring several times in a set of calculations. Correspondingly, the greater the number of occurrences of this minimum, the greater the confidence in it being global, although this is no guarantee. The number of calculations performed for each potential for each value of N and the number of occurrences of the lowest energy structure are given in table 1. The inefficiency of this approach is obvious, but appears necessary if results from other calculations are to be verified, and provides a yardstick by which other methods can be compared. In this model, atoms are treated independently, allowed to interact freely and the minimum energy geometry solved globally rather than locally. That a global minimum is difficult to find is a measure of the magnitude of the problem, not a deficiency of the approach.

The geometries calculated for the two "harder" potentials show a tendency for the formation of pockets of local fivefold symmetry. The "soft" potential, on the other hand, was less likely to form structures in which the dominant symmetry was fivefold, but often contained many five-coordinate atoms. In particular, the icosahedron played an important part in the prevalent geometries, providing a structural building block around which many structures were based. Pertinent examples of this were the structures for $N = 13, 23, 26$ and 29, for which the same polyicosahedral structures were calculated for each potential function used.

Perhaps the biggest problem with the use of these potential functions is their tendency to encourage "bond" formation and, as a result, overestimating the number of nearest-neighbour contacts present in a structure. Cluster geometries calculated using the 12–6 potential do agree with those observed for noble gas clusters [35], but are less successful for other cluster types [30]. A good example of this can be seen in the Pt_{19} structure, which is a {1, 5, 1, 5, 1, 5, 1} polyhedron and not a double-icosahedron as calculated using the 12–6 potential [31].

Table 1

A summary of the number of calculations performed, the number of times a global minimum energy structure was found, and that energy. The column N gives the number of atoms in the cluster, T is the number of calculations performed for that value of N, F is the number of times the lowest energy structure was found, and $|E|$ is the (positive) value of that lowest energy.

	Results for the 2–1 potential calculations			Results for the 8–4 potential calculations			Results for the 12–6 potential calculations[a]		
N	T	F	$\|E\|$	T	F	$\|E\|$	T	F	$\|E\|$
3	50	50	3.0000	50	44	3.0000	50	38	3.0000
4	50	50	6.0000	50	43	6.0000	50	40	6.0000
5	50	50	9.8767	50	43	9.2685	50	39	9.1039
6	50	50	14.7712	50	45	13.3385	50	6	12.7121
7	50	50	20.4190	50	11	17.3579	50	9	16.5054
8	50	50	27.0120	50	28	21.5536	50	13	19.8215
9	50	46	34.4867	50	7	26.1769	50	3	24.1134
10	50	24	42.7733	50	7	31.2964	50	4	28.4225
11	50	50	52.0787	50	15	36.6089	50	2	32.7660
12	50	48	62.1683	50	22	42.9844	50	2	37.9676
13	100	100	73.3566	100	42	50.4208	100	4	44.3268
14	100	100	84.9749	100	72	55.0978	100	9	47.8451
15	100	100	97.6125	100	27	60.7825	100	4	52.3226
16	100	95	110.9957	100	23	66.6609	100	3	56.8157
17	100	63	125.2110	100	3	72.7205	500	1	61.3180
18	100	68	140.1846	100	10	79.6984	250	1	66.5309
19	100	70	156.1240	500	64	87.4067	500	2	72.6598
20	100	64	172.8500	200	40	93.7617	200	3	77.1770
21	100	35	190.3933	250	3	99.9702	250	2	81.6846
22	100	40	208.7537	200	23	107.3897	200	1	86.8097
23	100	27	228.0988	100	9	115.6053	500	1	92.8445
24	100	83	248.1847	200	21	122.2177	200	1	97.3488
25	100	77	269.0686	200	20	129.6841	700	1	102.3727
26	100	80	290.8581	200	12	138.2707	1250	0	108.3156[b]
27	100	12	313.1490	100	6	144.9548	1250	1	112.8736
28	100	32	336.4765	100	6	152.4361	500	1	117.8224
29	100	6	360.6191	200	3	161.0145	1000	0	123.5873[b]
30	100	88	385.6844	300	2	167.9429	2500	0	128.1816[c]
31	100	80	411.3207	200	3	175.5241	1000	0	133.5864[d]
32	100	66	437.8247	200	7	184.1283	1000	0	139.6355[d]
33	100	26	465.2363	100	4	191.8851	1000	0	144.8427[d]
34	100	42	493.2831	300	6	200.6877	1500	0	149.9970[c]
35	100	38	522.1111	300	7	207.8171	1500	0	155.0781[c]
36	100	37	551.7809	200	2	215.7403	500	0	160.8384[c]
37	100	36	582.2931	400	1	224.1307	500	0	166.9130[c]
38	100	30	613.6250	300	1	232.2865	500	0	172.2006[c]
39	100	52	645.7353	400	1	241.1656			
40	300	130	678.6294	500	4	249.6569			

[a] Energies quoted, unless marked otherwise, are the same as those calculated by Northby [19].

[b] The lowest energy structure found from the 8–4 potential calculation was used as a starting approximation to calculate this structure.

[c] The energy given is the lowest value calculated in this work. This energy is higher than that obtained using a lattice-based search and optimisation procedure [19].

[d] The lowest energy structure was not found after the quoted number of calculations using random starting approximations were performed. Instead, the structure obtained by minimising either an $N + 1$ or $N - 1$ starting approximation gave a structure of lowest energy.

Another example of the failure to reproduce known chemical structure is the R105 structure of boron [36] which, although polyicosahedral, is less compact than that calculated using the 12–6 potential and was not found even as a local minimum. Other examples are the structures of $N = 37$ and 38 clusters [30,32] containing both gold and silver atoms. These clusters are made up of vertex-sharing icosahedra but are not as compact as the structures anticipated using the method described here. Instead, each of these clusters may be better considered as "cluster of clusters" (or supracluster) [30], which would require a more complex set of potential functions if they were to be modelled.

The potential functions employed in this work ignore the effects of many-body interactions. They may not affect ground-state geometries [17], but their inclusion is important if a more realistic model is to be developed [37]. However, the simplicity afforded by the neglect of such interactions enables the problem to be kept computationally simple. Of perhaps more importance to this work is the need for calibration of the calculated energies in order to assess the real difference in energies between structures and the extent to which a structure can be less energetically favourable than the lowest calculated yet still be plausible.

The basic model has been extended to describe the geometries of clusters containing two different types of atom. There are other ways in which these clusters could be modelled which take into account the physical properties of the atoms making up the cluster, for example a pair potential incorporating charge has been used to model small clusters of $[Ti_nO_{2n-1}]^+$ [38]. Bimetallic clusters have been modelled using intermolecular potentials which include terms accounting for the electron densities of the different atoms [34], and water-ion clusters have been modelled using non-additive intermolecular potentials [39].

It is also possible that three-body interactions may assume greater importance in X_xY_y clusters. Superficially, one can imagine that there might be a greater third body interaction due to one of the atoms compared to the other, which may influence the geometry of the molecule. It has been shown that three-body interactions are significant for certain geometries of aromatic–rare gas clusters [40] and the assumption that they do not affect the ground-state geometry of (X only) N atom clusters [17] may not be valid for X_xY_y clusters.

Despite the simplicity of the model used in the calculations for X_xY_y clusters when compared to these more complex types of calculation, interesting and valuable results have been obtained. The polyicosahedral structures calculated to be global minima for X_x clusters are not necessarily valid for those of the type X_xY_y, especially when the difference in the sizes of X and Y is large. Another general conclusion gained from this work is that the smaller atoms tend to congregate in the interior of the cluster. The formation of a subcluster of smaller atoms surrounded by a shell consisting of the larger atoms can be seen in all of the minimum energy clusters calculated in this work. Furthermore, these core polyhedra may not be the same as those calculated when the enclosed atoms are of the same type as those on the cluster surface.

This work demonstrates the dependence of cluster geometry on the type of functions used to model atom–atom interactions, and also its dependence on the relative sizes of the constituent atoms. Some results obtained previously [19] have been verified without making a priori assumptions as to the most probable outcome and new structures, for both soft-packed and substituted clusters, have been found.

Acknowledgements

This work was supported by the Australian Research Council. One of us (I.B.) is grateful for the financial assistance provided in the form of a Commonwealth Postgraduate Research Allowance.

References

[1] C.A. Rodgers, Proc. London Math. Soc. (3) 8(1958)609.
[2] A.H. Boerdijk, Philips Res. Rep. 7(1952)303.
[3] A.L. Mackay, Acta Cryst. 15(1962)916.
[4] J.G. Allpress and J.V. Sanders, Surface Sci. 7(1967)1.
[5] Y. Fukano and C.M. Wayman, J. Appl. Phys. 40(1969)1656.
[6] J.G. Allpress and J.V. Sanders, Aust. J. Phys. 23(1970)23.
[7] J.J. Burton, Nature 229(1971)335.
[8] J.D. Bernal, Nature 185(1959)141.
[9] G. Mason and W. Clark, Nature 207(1965)512.
[10] G. Mason and W. Clark, Nature 211(1966)957.
[11] J.D. Bernal and S.V. King, Faraday Disc. Chem. Soc. 43(1967)60.
[12] J.D. Bernal and J.L. Finney, Faraday Disc. Chem. Soc. 43(1967)62.
[13] M.R. Hoare and P. Pal, Adv. Phys. 20(1971)161.
[14] M.R. Hoare and P. Pal, Nature 230(1971)5.
[15] M.R. Hoare and J. McInnes, Faraday Disc. Chem. Soc. 61(1976)12.
[16] M.R. Hoare, Adv. Chem. Phys. 40(1979)49.
[17] L.T. Wille, Chem. Phys. Lett. (1987) 133; 405.
[18] J. Uppenbrink and D.J. Wales, J. Chem. Soc. Faraday Trans. 87(1991)215.
[19] J.A. Northby, J. Chem. Phys. 87(1987)6166.
[20] W.C. Davidson, Math. Prog. 9(1975)1.
[21] B.W. Clare, M.C. Favas, D.L. Kepert and A.S. May, Adv. Dyn. Stereochem. 1(1985)1.
[22] M.C. Favas, *The MINIM Subroutine* (University of Western Australia, 1985).
[23] B.W. Clare and D.L. Kepert, Proc. Roy. Soc. London A405(1986)329.
[24] N.R. Taylor, Ph.D. Thesis, University of Western Australia (1990).
[25] D.J. Fuller and D.L. Kepert, Inorg. Chem. 21(1982)163.
[26] B.W. Clare and D.L. Kepert, Inorg. Chem. 23(1984)1521.
[27] B.W. Clare and D.L. Kepert, Polyhedron 6(1987)619.
[28] H.M. Cundy and A.P. Rollet, *Mathematical Models*, 2nd ed. (Oxford University Press, Oxford, 1974).
[29] J.D. Bernal, Proc. Roy. Soc. A280(1964)299.
[30] B.K. Teo, M.C. Hong, H. Zhang and D.B. Huang, Angew. Chem. Int. Ed. Engl. 26(1987)897.
[31] D.M. Washecheck, E.J. Wucherer, L.F. Dahl, A. Ceriotti, G. Longoni, M. Mamassero, M. Sansoni and P. Chini, J. Amer. Chem. Soc. 101(1979)6110.

[32] B.K. Teo, H. Zhang and X. Shi, J. Amer. Chem. Soc. 112(1990)8552.
[33] B.K. Teo and K. Keating, J. Amer. Chem. Soc. 106(1984)2224.
[34] M.S. Stave, D.E. Sanders, T.J. Raeker and A.E. DePristo, J. Chem. Phys. 93(1990)4413.
[35] J. Farges, M.F. de Feraudy, B. Raoult and G. Torchet, J. Chem. Phys. 78(1983)5067.
[36] J. Donohue, *The Structures of the Elements* (Wiley–Interscience, New York, 1974).
[37] D.J. Wales, J. Amer. Chem. Soc. 112(1990)7908.
[38] Wen Yu and R.B. Freas, J. Amer. Chem. Soc. 112(1990)7126.
[39] J. Caldwell, L.X. Dang and P.A. Kollman, J. Amer. Chem. Soc. 112(1990)9144.
[40] A.T. Amos, T.F. Palmer, A. Walters and B.L. Burrows, Chem. Phys. Lett. 172(1990)503.